Nanoscale Research Letters
a SpringerOpen Journal

NANO EXPRESS Open Access

Synthesis and optical property of one-dimensional spinel $ZnMn_2O_4$ nanorods

Pan Zhang[1†], Xinyong Li[1,2*†], Qidong Zhao[1†] and Shaomin Liu[2*†]

Abstract

Spinel zinc manganese oxide ($ZnMn_2O_4$) nanorods were successfully prepared using the previously synthesized α-MnO_2 nanorods by a hydrothermal method as template. The nanorods were characterized by X-ray diffraction, scanning electron microscopy, transmission electron microscopy, UV-Vis absorption, X-ray photoelectron spectroscopy, surface photovoltage spectroscopy, and Fourier transform infrared spectroscopy. The $ZnMn_2O_4$ nanorods in well-formed crystallinity and phase purity appeared with the width in 50-100 nm and the length in 1.5-2 μm. They exhibited strong absorption below 500 nm with the threshold edges around 700 nm. A significant photovoltage response in the region below 400 nm could be observed for the nanorods calcined at 650 and 800° C.

Introduction

Spinel is an important class of mixed-metal oxides, which has the general chemical composition of AB_2O_4. In recent years, mixed transition-metal oxides with spinel structure have attracted much attention, owing to their various properties such as photocatalytic [1-4], electrochemical performance [5], magnetic [6,7] properties, or being used as lithium ion batteries [8]. Mn-doped ZnO has also aroused lots of interest because it had been predicted to be a room-temperature diluted magnetic semiconductor [9], which was later verified by experiments. Therefore, the Mn-Zn-O ternary systems belong to a class of interesting and useful materials in terms of their electrical and magnetic properties.

As one of the important mixed transition-metal oxides with spinel structure, $ZnMn_2O_4$ is a promising functional material and has become the focus of various researches owing to its potential applications. $ZnMn_2O_4$ could be used for the negative temperature coefficient thermistors on account of their unique electrical properties [10]. Ferrari and the coworkers studied the catalytic activity of zinc manganite for the reduction of NO by several types of hydrocarbons [4,11]. Those authors suggested that $ZnMn_2O_4$ was an efficient catalyst for the reduction of NO to N_2, and, in all cases, its best selectivity to N_2 and CO_2 was at almost the maximum conversion temperature.

The physical and chemical properties of nanomaterials would be strongly affected by their particle sizes and morphologies [12]. At present, a tremendous amount of comprehensive investigations are under way into the unique applications of one-dimensional (1D) nanostructures involving nanorods, nanotubes, nanowires, and nanobelts because they provide a great opportunity to investigate the dependence of optical/electrical properties, thermal transport, and mechanical performance on the nano-scaled dimensionality and size [13,14]. 1D nanomaterials, especially nanorods have displayed enhanced performances in many fields such as catalysts [15], sensors [9], solar cells [16], and so on.

$ZnMn_2O_4$ particles could be prepared earlier by various methods, such as solid-state reaction [17,18], sol-gel [19], co-precipitation method [18], and hydrothermal method [20,21]. For instance, Bessekhouad and Trari [18] prepared spinel $ZnMn_2O_4$ powder by solid-state reaction under high temperature. Zhang et al. [21] fabricated $ZnMn_2O_4$ nanoparticles by a hydrothermal method expending 48 h. Fan et al. [22] successfully synthesized 1D single-crystalline spinel MFe_2O_4 nanotubes/nanorings by thermal transformation process. In this study, we prepare the $ZnMn_2O_4$ nanorods

* Correspondence: xyli@dlut.edu.cn; shaomin.liu@curtin.edu.au
† Contributed equally
[1]Key Laboratory of Industrial Ecology and Environmental Engineering and State Key Laboratory of Fine Chemical, School of Environmental Science & Technology, Dalian University of Technology, Dalian, 116024, China
[2]Department of Chemical Engineering, Curtin University, Perth, WA 6845, Australia
Full list of author information is available at the end of the article

successfully using the α-MnO_2 nanorods as templates. The $ZnMn_2O_4$ nanorods obtained thus are well characterized, demonstrating their morphology, optical, and photoelectric properties.

Experimental

Synthesis

All chemicals used in this study were analytic-grade reagents and used without further purification. At first, α-MnO_2 nanorods were prepared by a hydrothermal approach. In a typical synthesis procedure, 0.8686 g $KMnO_4$ and 1.8 mL concentrated HCl (37 wt%) were added to 100 mL deionized water to form the precursor solution, which was then transferred into a Teflon-lined stainless steel autoclave with a capacity of 120 mL. The autoclave was sealed and hydrothermally treated at 140°C for 12 h. After the autoclave was cooled down to room temperature naturally, the black precipitates were collected by centrifugation and washed with deionized water and anhydrous ethanol several times to remove possible impurities or excess ions. The as-prepared sample was then dried in air overnight.

To obtain $ZnMn_2O_4$ nanorods, the prepared α-MnO_2 nanorods (0.0174 g) were placed in 20 mL distilled water at room temperature to form a mixed solution by constant stirring. A $Zn(NO_3)_2$ solution (2.5 mL, 0.1 M) was then added to the solution, which was continually stirred for 5 min. Then NaOH solution (40 mL, 0.1 M) was directly added to the above solution dropwise, and the resulting mixture was maintained for 30 min under continuous stirring. The base-treated products were washed with distilled water and anhydrous ethanol several times. Next, the products were all calcined at 500, 550, 600, 650, and 800°C for 2 h in air.

Characterizations

The crystal structures and microstructures of the products were characterized by X-ray diffraction (XRD) (D/MAX-2400). The chemical composition of the samples was crosschecked by energy dispersive X-ray spectroscope (EDS, JSM-5600LV). The SEM (Quanta 200 FEG), transition electron microscopy (TEM)/high-resolution transition electron microscopy (HRTEM) (JEOL JEM-2000EX), and selected area electron diffraction (SAED, Tecnai G220) were employed to observe the samples morphology. UV-Vis spectrophotometer (JASCO, UV-550) and a home-built surface photovoltage (SPV) measurement system based on a lock-in amplifier (Stanford, SR830) were employed to test the optical and photoelectric properties. X-ray photoelectron spectroscopy (XPS, PHI 5600) was employed to reveal the surface chemical composition of the products. The chemical compositions of the different products were determined using Fourier transform infrared spectroscopy (FTIR, VERTEX 70).

Results and discussion

XRD patterns of the calcined samples

The crystallinities and phase purities of the $ZnMn_2O_4$ nanorods calcined were examined by powder XRD. Figure 1 shows the XRD patterns of the samples after calcination at different temperatures and as per the standard data card about the $ZnMn_2O_4$. After calcination at 650°C, all the XRD peaks of the calcined samples could be indexed to cubic $ZnMn_2O_4$ with spinel structure (JCPDS file No.24-1133), where the diffraction peaks at 2θ values of 29.3°, 33.03°, 36.3°, 59.01°, 60.77°, and 65.1° are ascribed to the reflection of (112), (103), (211), (321), (224), and (400) planes of the spinel $ZnMn_2O_4$, respectively. No peaks from other phases are detected, indicating high purity of the products. However, in the products which were calcined at 500°C, the diffraction peaks of α-MnO_2 and ZnO could still be seen clearly, implying that the precursor was not converted into spinel $ZnMn_2O_4$ completely even at such a calcination temperature. As for the sample treated at 800°C, two peaks of α-MnO_2 preferential growth along (110) and (220) crystal faces at the surface of $ZnMn_2O_4$ nanorods were detected again because of partial decomposition of $ZnMn_2O_4$. Meanwhile, the peaks of α-MnO_2 and ZnO could also be seen unambiguously when the precursors were calcined at 550 and 600°C (see Figure S1 in Additional file 1). These phenomena indicate that the formation of $ZnMn_2O_4$ began at the calcination temperature of about 650°C. On increasing the calcination temperature from 500 to 800°C, the peak widths of the $ZnMn_2O_4$ nanorods become narrower, and the relative intensities of the characteristic peaks increase gradually, which implies that the spinel $ZnMn_2O_4$ crystallites were growing and transforming from the disordered to a more ordered structure [23].

SEM images and elemental analysis of the nanorods

The general morphology of these nanorods was observed using scanning electron microscopy (SEM). Figure 2a displays an overview image of the α-MnO_2 nanorods. After coating $Zn(OH)_2$ onto the α-MnO_2 nanorods, the precursor of $ZnMn_2O_4$ nanorods is obtained. The SEM images in Figure 2b show that the morphology does not change with the rod width in the range of 50-100 nm and the length in the range of 1.5-2 μm. The morphology of the $ZnMn_2O_4$ obtained by calcination at 650°C of the precursor is shown in Figure 2c. It also displays a similar morphology to the MnO_2 nanorods. The EDS characterization at the same position was carried out. As shown in Figure 2d, it is clear that the nanorods consist of Zn, Mn, and O and the elemental ratio of Zn to Mn is determined to be about 1:2.

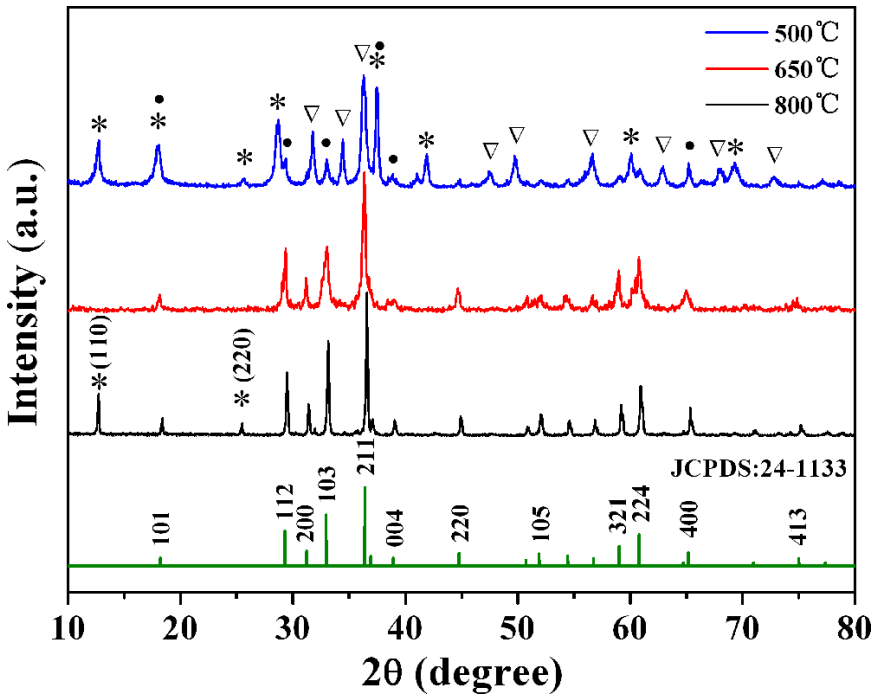

Figure 1 XRD patterns of the $ZnMn_2O_4$ nanorods at different calcined temperatures and as per the standard card about $ZnMn_2O_4$ (JCPDS file No.24-1133). Asterisks, α-MnO_2; inverted triangle, ZnO; filled circle, $ZnMn_2O_4$.

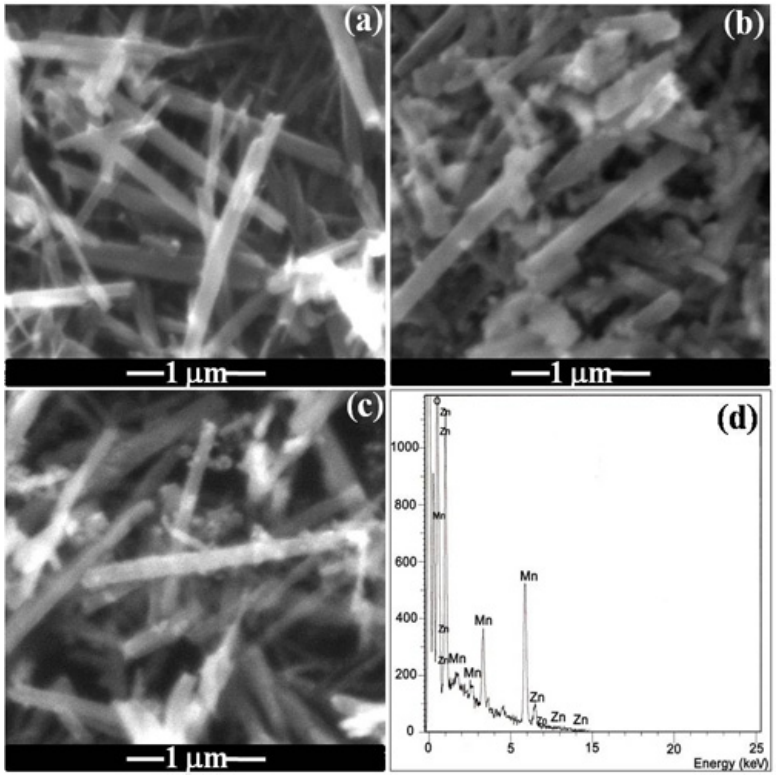

Figure 2 The SEM images of different samples: **(a)** α-MnO_2 nanorods; **(b)** α-MnO_2/$Zn(OH)_2$ nanorods; **(c)** the $ZnMn_2O_4$ nanorods calcined at 650°C; and **(d)** EDS spectrum of the $ZnMn_2O_4$ nanorods calcined at 650°C.

TEM and HRTEM images of the $ZnMn_2O_4$ nanorods

The TEM and HRTEM were employed to further investigate the morphology of these nanocrystalline $ZnMn_2O_4$ superstructures calcined at 650°C (Figure 3). TEM image confirms the nanocrystalline feature of the $ZnMn_2O_4$ particles (Figure 3a,b), in which the individual rod width is in the range of 50-100 nm. Figure 3c shows the HRTEM image of $ZnMn_2O_4$ nanorods. The inset in Figure 3c is the enlargement of the selected area, indicating the good crystallization of the nanoparticles. The fringes of d = 0.246 nm match that of the (211) crystallographic plane of $ZnMn_2O_4$, which is the strongest crystallographic plane, corresponding to the distance between (211) crystal planes of the spinel phase of zinc manganese oxide (JCPDS file No. 24-1133). Figure 3d is the SAED image of the $ZnMn_2O_4$ nanorods, which shows the (211), (224), and (321) crystal planes clearly.

The UV-Vis diffuse reflectance spectra of the $ZnMn_2O_4$ nanorods

The optical property of the $ZnMn_2O_4$ nanorods can be observed by the UV-Vis diffuse reflectance spectroscopy. Figure 4a shows the UV-Vis diffuse reflectance spectra of the $ZnMn_2O_4$ nanorods calcined at different temperatures. All the samples have strong absorption between 300 and 500 nm, and the absorption edges of these samples are all around 700 nm. The optical band gaps could be determined from the curves of $(\alpha h\upsilon)^n$ versus $h\upsilon$, α being the optical absorption coefficient. The exponent n equals 1/2 for indirectly allowed and 2 for directly allowed transitions (Figure 4). Figure 4b is the $(\alpha h\upsilon)^2$-$h\upsilon$ curves for the $ZnMn_2O_4$ nanorods calcined at different temperatures. The optical band gaps are calculated as 1.2, 1.34, and 1.45 eV for the samples calcined at 500, 650 and 800°C, respectively. No linear relation was found for n = 1/2, suggesting that the prepared $ZnMn_2O_4$ may be a semiconductor allowing direct transitions at these energy levels [3].

XPS spectra of the $ZnMn_2O_4$ nanorods

In $ZnMn_2O_4$, Mn and Zn atoms exist in the samples with more than one chemical state (A-sites or B-sites), bringing about several contributions with different binding energies in the XPS. Therefore, XPS was employed

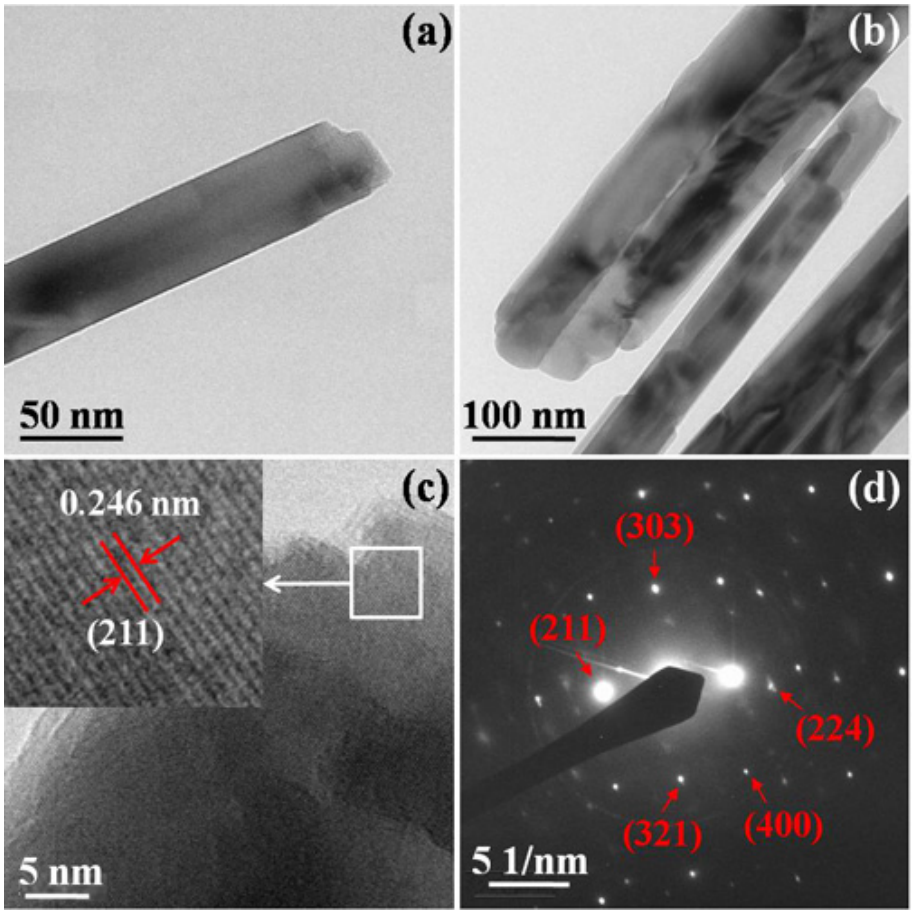

Figure 3 Characterization of the $ZnMn_2O_4$ nanorods calcined at 650°C: **(a,b)** TEM images; **(c)** HRTEM image. Inset: the enlargement of the marked square; and **(d)** SAED pattern.

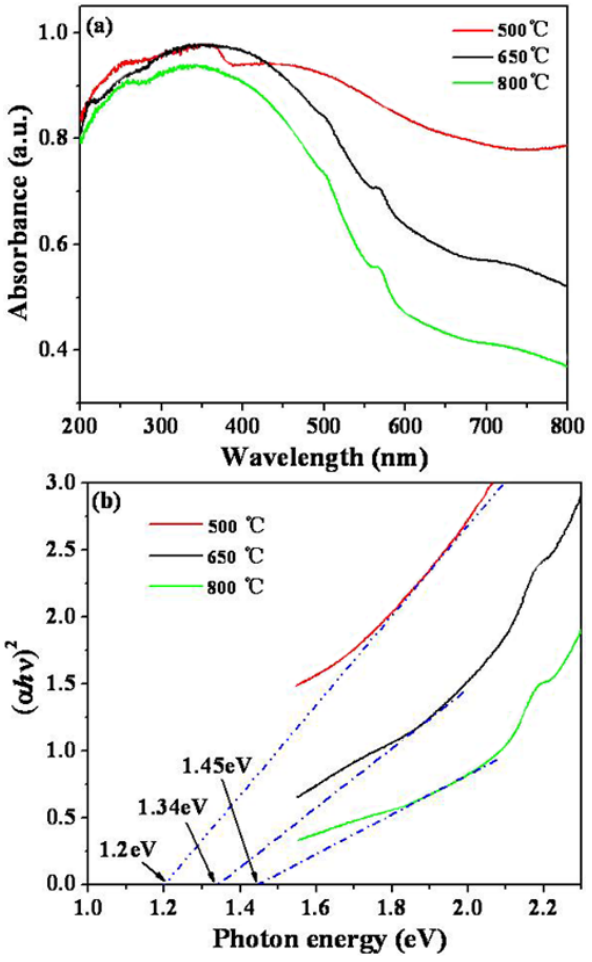

Figure 4 UV-Vis spectra and plots for band gaps determination. **(a)** The UV-Vis diffuse reflectance spectra of the $ZnMn_2O_4$ nanorods calcined at 500, 650, and 800°C, respectively; **(b)** plots of $(\alpha h\upsilon)^2$ versus photon energy of $ZnMn_2O_4$ nanorods calcined at 500, 650, and 800°C, respectively.

to reveal the surface chemical compositions of the nanocrystalline $ZnMn_2O_4$ superstructures obtained from the calcinations of the precursor at 650°C (Figure 5). Figure 5a shows the survey spectra of the nanocrystalline $ZnMn_2O_4$. Elements of Zn, Mn, O, and adventitious C existed in the $ZnMn_2O_4$. The carbonate species adsorbed on the surface have appeared from the calibration for XPS instrument itself. As shown in the spectrum in Figure 5b, the peaks of 654.4 and 642.4 eV can be attributed to Mn $2p_{1/2}$ and Mn $2p_{3/2}$, respectively. Figure 5c shows the Zn 2*p* peaks at binding energies of 1044.8 and 1021.6 eV. This reveals the oxidation state of Mn^{3+} in the sample. Meanwhile, O 1s spectra of $ZnMn_2O_4$ were also recorded (Figure 5d). The broad peak of O 1s can be fitted by two peaks at binding energies of 531.8 and 530.2 eV. The stronger peak at 530.2 eV is ascribed to the characteristics of oxygen in metal oxide, and the other peak at around 531.8 eV suggests the presence of other components, such as OH, H_2O, and carbonate species adsorbed on the surface. In addition, XPS analysis confirms that the ratio of Zn to Mn in the sample is very close to 1:2, which is in good agreement with the formula of $ZnMn_2O_4$.

SPV spectra of the $ZnMn_2O_4$ nanorods

SPV method, a well-established technique for the characterization of photoelectric materials, can be used to investigate their photoelectric properties [24]. Figure 6 presents the obtained SPV amplitude spectra for the $ZnMn_2O_4$ nanorods calcined at 500, 650, and 800°C and the schematic of the AC photovoltaic cells. As the calcined temperature goes on increasing, the SPV response intensities become stronger and stronger because the spinel $ZnMn_2O_4$ nanorods become well ordered and the crystallinities enhance. For the $ZnMn_2O_4$ nanorods calcined at 650 and 800°C, a significant SPV response band could be observed in the region 300-400 nm, which is directly related to the free charge carriers induced by the incident light. However, only a very small response can be observed about the product calcined at 500°C because of poor crystallinity of $ZnMn_2O_4$ as well as the existence of α-MnO_2, which almost cannot produce SPV response.

IR spectra of the $ZnMn_2O_4$ nanorods

Infrared (IR) spectroscopy could provide plentiful information on the molecular structure and chemical bonding, which enables the characterization and identification of chemical species. Herein, we employed IR spectroscopy to comparatively analyze and identify the material compositions of different products. The IR spectra of the prepared samples treated at 500, 650, and 800°C are presented in Figure 7. The spectrum of the precursor calcined at 500°C shows a band at 531 cm^{-1}, which is attributed to the Mn-O vibrations of MnO_2. The bands belonging to $ZnMn_2O_4$ nanorods are considerably weak, probably because of the co-existence of α-MnO_2 and ZnO. When the temperature reached 650°C, a strong band at 516 cm^{-1} and a weak one at 623 cm^{-1} related to spinel $ZnMn_2O_4$ appear. Upon increasing the treatment temperature to 800°C, these bands become more intense and shift to higher wavenumbers, from 516 to 547 cm^{-1} and from 623 to 642 cm^{-1}, which reveals the formed spinel nanorods have achieved an improved crystallinity [25].

Conclusions

In summary, one-dimensional spinel $ZnMn_2O_4$ nanorods were successfully fabricated using the α-MnO_2 nanorods as template. The $ZnMn_2O_4$ nanorods mainly grew along the (211) crystalline plane with the width in

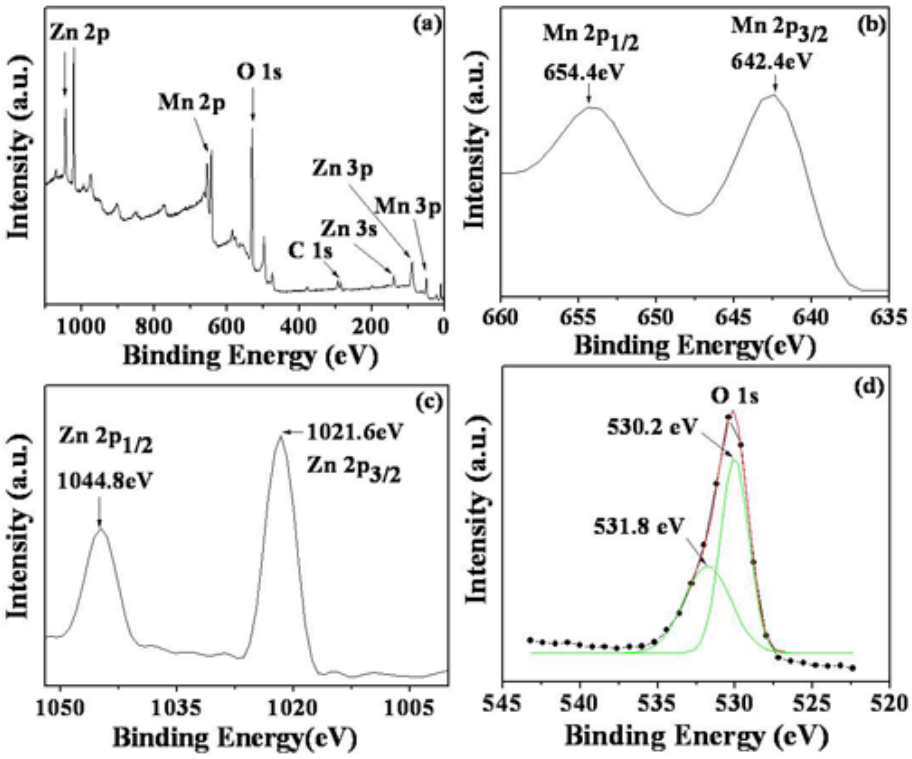

Figure 5 XPS spectra of the $ZnMn_2O_4$ nanorods obtained by calcining the precursor at 650°C: **(a)** survey of the sample; **(b)** Mn 2p; **(c)** Zn 2p; and **(d)** O 1s.

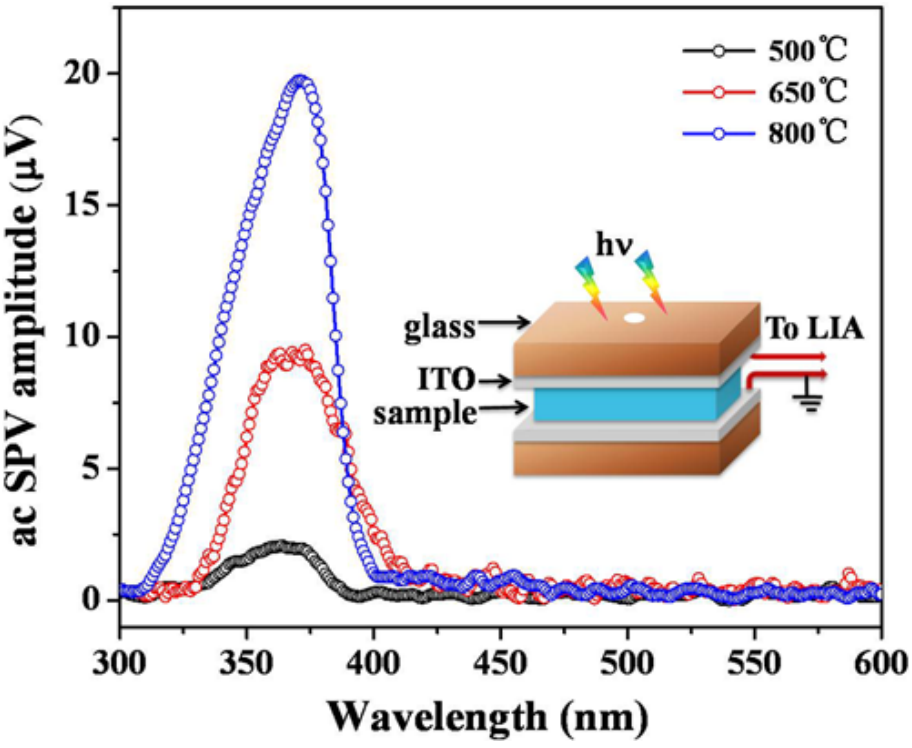

Figure 6 AC SPV amplitude spectra of the $ZnMn_2O_4$ nanorods calcined at 500, 650, and 800°C. Inset: schematic of the AC photovoltaic cells.

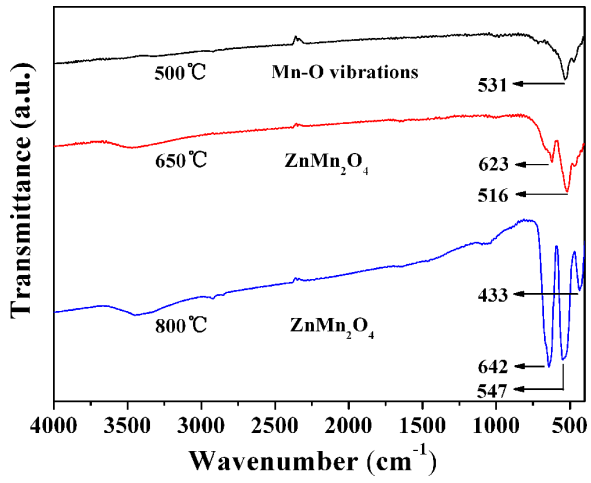

Figure 7 FTIR spectra for the $ZnMn_2O_4$ nanorods calcined at 500, 650, and 800°C, respectively.

50-100 nm and the length in 1.5-2 μm. The optical band gap energies of the nanorods calcined at 500°C, 650°C, and 800°C were respectively estimated to be 1.2, 1.34, and 1.45 eV. As the calcination temperature increased, they presented with much improved crystallinity and photoelectric response. The simple method for preparing the $ZnMn_2O_4$ nanorods reported here could also be utilized to fabricate other manganates.

Additional material

Additional file 1: Figure S1 XRD patterns of the $ZnMn_2O_4$ nanorods calcined at different temperatures. *Asterisks, α-MnO_2; inverted triangle, ZnO; filled circle, $ZnMn_2O_4$.

Abbreviations

EDS: energy dispersive X-ray spectroscope; FTIR: Fourier transform infrared spectroscopy; HRTEM: high-resolution transition electron microscopy; SAEDL: selected area electron diffraction; SPV: surface photovoltage; TEM: transition electron microscopy; XPS: X-ray photoelectron spectroscopy; XRD: X-ray diffraction.

Acknowledgements

This study was supported financially by the National Nature Science Foundation of China (No. 20877013, NSFC-RGC 21061160495), the National High Technology Research and Development Program of China (863 Program) (No. 2007AA061402), the Major State Basic Research Development Program of China (973 Program) (No. 2007CB613306), and the Excellent Talents Program of Liaoning Provincial University (LR2010090).

Author details

[1]Key Laboratory of Industrial Ecology and Environmental Engineering and State Key Laboratory of Fine Chemical, School of Environmental Science & Technology, Dalian University of Technology, Dalian, 116024, China
[2]Department of Chemical Engineering, Curtin University, Perth, WA 6845, Australia

Authors' contributions

PZ conceived of the study, carried out the experiment process, did the most parts' characterizations, and drafted the manuscript. XYL conceived of the study, guided the research, and helped in drafting the manuscript. QDZ and SML participated in research coordination, draft revision, and helped in drafting the manuscript. All the authors read and approved the final manuscript.

Competing interests

The authors declare that they have no competing interests.

Received: 23 December 2010 Accepted: 11 April 2011
Published: 11 April 2011

References

1. Xu SH, Feng DL, Shangguan WF: **Preparations and photocatalytic properties of visible-light-active zinc ferrite-doped TiO_2 photocatalyst.** *J Phys Chem C* 2009, **113**:463-2467.
2. Ding DW, Long M, Cai WM, Wu YH, Wu DY, Chen C: **In situ synthesis of photocatalytic $CuAl_2O_4$-Cu hybrid nanorod arrays.** *Chem Commun* 2009, **24**:3588-3590.
3. Cui B, Lin H, Liu YZ, Li JB, Sun P, Zhao XC, Liu CJ: **Photophysical and photocatalytic properties of core-ring structured $NiCo_2O_4$ Nanoplatelets.** *J Phys Chem C* 2009, **113**:14083-14087.
4. Fierro G, Jacono ML, Dragone R, Ferraris G, Andreozzi GB, Graziani G: **Fe-Zn manganite spinels and their carbonate precursors: preparation, characterization and catalytic activity.** *Appl Catal B Environ* 2005, **57**:153-165.
5. Tian L, Yuan AB: **Electrochemical performance of nanostructured spinel $LiMn_2O_4$ in different aqueous electrolytes.** *J Power Sources* 2009, **192**:693-697.
6. Chen JP, Sorensen CM: **Size-dependent magnetic properties of $MnFe_2O_4$ fine particles synthesized by coprecipitation.** *Phys Rev B* 1996, **54**:9288-9296.
7. Blanco-Gutiérrez V, Torralvo-Fernández MJ, Sáez-Puche R: **Magnetic behavior of $ZnFe_2O_4$ nanoparticles: effects of a solid matrix and the particle size.** *J Phys Chem C* 2010, **114**:1789-1795.
8. Yang YY, Zhao YQ, Xiao LF, Zhang LZ: **Nanocrystalline $ZnMn_2O_4$ as a novel lithium-storage material.** *Electrochem Commun* 2008, **10**:1117-1120.
9. Dietl T, Ohno H, Matsukura F, Cibert J, Ferrand D: **Zener model description of ferromagnetism in zinc-blende magnetic semiconductors.** *Science* 2000, **287**:1019-1022.
10. Guillemet-Fritsch S, Chanel C, Sarrias J, Bayonne S, Rousset A, Alcobe X, Martinez Sarriòn ML: **Structure, thermal stability and electrical properties of zinc manganites.** *Solid State Ionics* 2000, **128**:233-242.
11. Ferraris G, Fierro G, Jacono ML, Inversi M, Dragone R: **A study of the catalytic activity of cobalt-zinc manganites for the reduction of NO by hydrocarbons.** *Appl Catal B Environ* 2002, **36**:251-260.
12. Barth S, Hernandez-Ramirez F, Holmes JD, Romano-Rodriguez A: **Synthesis and applications of one-dimensional semiconductors.** *Prog Mater Sci* 2010, **55**:563-627.
13. Xia YN, Yang PD, Sun YG, Wu YY, Mayers B, Gates B, Yin YD, Kin F, Yan HQ: **One-dimensional nanostructures: synthesis, characterization, and applications.** *Adv Mater* 2003, **15**:353-389.
14. Wang ZL: **Characterizing the structure and properties of individual wire-like nanoentities.** *Adv Mater* 2000, **12**:1295-1298.
15. Shi R, Wang YJ, Li D, Xu J, Zhu YF: **Synthesis of $ZnWO_4$ nanorods with [100] orientation and enhanced photocatalytic properties.** *Appl Catal B Environ* 2010, **100**:173-178.
16. Yu KH, Chen JH: **Enhancing solar cell efficiencies through 1-D nanostructures.** *Nanoscale Res Lett* 2009, **4**:1-10.
17. Peiteado M, Caballero AC, Makovec D: **Diffusion and reactivity of ZnO-MnOx system.** *J Solid State Chem* 2007, **180**:2459-2464.
18. Bessekhouad Y, Trari M: **Photocatalytic hydrogen production from suspension of spinel powders AMn_2O_4 (A = Cu and Zn).** *Int J Hydrogen Energy* 2002, **27**:357-362.
19. Peng HY, Wu T: **Nonvolatile resistive switching in spinel $ZnMn_2O_4$ and ilmenite $ZnMnO_3$.** *Appl Phys Lett* 2009, **95**:152106-152106.
20. Xiao LF, Yang YY, Yin J, Li Q, Zhang LZ: **Low temperature synthesis of flower-like $ZnMn_2O_4$ superstructures with enhanced electrochemical lithium storage.** *J Power Sources* 2009, **194**:1089-1093.
21. Zhang XD, Wu SZ, Zang J, Li D, Zhang ZD: **Hydrothermal synthesis and characterization of nanocrystalline Zn-Mn spinel.** *J Phys Chem Solids* 2007, **68**:1583-1590.

22. Fan HM, Yi JB, Yang Y, Kho KW, Tan HR, Shen ZX, Ding J, Sun XW, Olivo MC, Feng YP: **Single-crystalline MFe_2O_4 nanotubes/nanorings synthesized by thermal transformation process for biological applications.** *ACS Nano* 2009, **3**:2798-2808.
23. Chen YC, Xie K, Pan Y, Zheng CM: **Effect of calcination temperature on the electro chemical performance of nanocrystalline $LiMn_2O_4$ prepared by a modified resorcinol-formaldehyde route.** *Solid State Ionics* 2010, **181**:1445-1450.
24. Kronik L, Shapira Y: **Surface photovoltage phenomena: theory, experiment, and applications.** *Surf Sci Rep* 1999, **37**:1-206.
25. Selim MM, Deraz NM, Elshafey OI, El-Asmy AA: **Synthesis, characterization and physicochemical properties of nanosized Zn/Mn oxides system.** *J Alloys Compd* 2010, **506**:541-547.

doi:10.1186/1556-276X-6-323
Cite this article as: Zhang *et al.*: Synthesis and optical property of one-dimensional spinel $ZnMn_2O_4$ nanorods. *Nanoscale Research Letters* 2011 **6**:323.